Growth of Graphite Nanofibers from the Iron−Copper Catalyzed Decomposition of CO/H_2 Mixtures

O. C. Carneiro,[†] M. S. Kim,[#] J. B. Yim,[#] N. M. Rodriguez,[†,‡] and R. T. K. Baker*[,†,‡]

Department of Chemistry, Northeastern University, Boston, Massachusetts 02115, and Division of Ceramic and Chemical Engineering, Myongji University, Yongin, Kyunggido, 449-728, Korea

Received: November 1, 2002

We have investigated the formation of graphite nanofibers from the catalytic decomposition of CO/H_2 mixtures over a series of powdered Fe−Cu catalysts at temperatures ranging from 500 to 700 °C. The physical and structural characteristics of the nanofibers have been established from examination of the materials by a variety of techniques including transmission electron microscopy, temperature-programmed oxidation, nitrogen surface area measurements, and X-ray diffraction. It was found that the addition of Cu to Fe did not exert a significant influence on the amount of solid carbon product formed in the reaction. On the other hand, examination of the nanofibers by high-resolution TEM revealed that the materials generated from Fe-rich Cu bimetallics were notably more graphitic in nature than those grown from pure Fe. As the reaction temperature was increased from 600 to 700 °C, the structure of the graphite nanofibers underwent a dramatic change from a "platelet" to "tubular" configuration. It is suggested that this transformation is directly associated with the α-Fe to γ-Fe phase change over this temperature range.

Introduction

In contrast to the iron subgroup transition elements, copper exhibits almost no activity with regard to catalytic formation of solid carbon when the metal is heated in the presence of either hydrocarbons or carbon monoxide. This behavior is related to the fact that copper does not dissociatively chemisorb these gases or dissolve carbon to any significant degree. These latter aspects are among the key steps involved the catalyzed growth of carbon structures.[1] On the other hand, when copper is combined with other metals it can exert a substantial promotional effect on the ability of the host to generate solid carbon formation during catalyzed decomposition of hydrocarbons.[2−5] Perhaps the best example of this effect is seen during the decomposition of a C_2H_4/H_2 (1:4) mixture at 600 °C over powdered iron catalysts containing various amounts of copper.[4] It was found that when either of the pure metals were reacted under these conditions very little catalytic activity was observed. A dramatic difference in behavior occurred, however, when the two metals were mixed together; the addition of a mere 2 wt % copper to iron resulted in a 20-fold increase in the amount of solid carbon product compared to that generated on pure iron at 600 °C. It was suggested that this behavior was related to the ability of copper to induce electronic perturbations in iron that were manifested in a change of the chemisorption properties of the surface atoms with respect to the hydrocarbon molecules.

The existence of a possible electronic factor in catalysis has been a topic of considerable controversy for many years.[6−8] The use of well-defined single-crystal surfaces has provided some new insights into the manner by which a small amount of an additive can modify the electronic properties of a host metal.[9,10] This work has led to the discovery that the strongest perturbations in a bimetallic system occur between combinations of "electron-rich" and "electron-poor" constituents.[11]

Copper−nickel has been used a model bimetallic system for numerous catalytic and surface science studies.[12−20] One can describe this system in terms of the electron-band theory, in which nickel is distinguished as having an incompletely filled d band, whereas that of copper is filled. When copper atoms are introduced into nickel extra electrons are added to the lattice, which enter the d-band until it is eventually completely filled. Varying the amount of copper that is added to the host metal can control the extent of d-band filling. Under these circumstances, one would predict that the catalytic properties of the bimetallic system would be very sensitive to the composition of the particles. Many researchers have emphasized that the surface composition of the bimetallic is likely to be significantly different to that of the bulk, and furthermore adsorption of certain gases could cause preferential surface segregation of one of the components.[21−23]

In the current investigation, we have studied the growth of graphite nanofibers generated during decomposition of CO/H_2 mixtures over powdered iron−copper catalysts at 500−700 °C. The formation of these types of solid structures imposes an intriguing set of demands on a bimetallic catalyst system. The first requirement is that the gaseous reactant encounters a metal surface where the crystallographic arrangement of the atoms favors the dissociative chemisorption of the carbon-containing molecules, but does not allow for the precipitation of any dissolved carbon atoms. This event must occur at a different set of crystallographic faces and if the metal−metal atom spacing at these regions is in register with that of the carbon−carbon distances in graphite then the ensuing nanofiber structure will possess a high degree of crystalline character. In this model, the rate-controlling step in the nanofiber growth process is bulk diffusion of carbon through the catalyst particle.[24,25]

A literature search reveals that various groups have studied the interaction of CO/H_2 mixtures with supported iron−copper

[†] Northeastern University.
[#] Myongji University.
[‡] Current address: Catalytic Materials LLC., West Holliston Professional Park, Holliston, MA 01746.

10.1021/jp022364e CCC: $25.00
Published on Web 04/15/2003

particles, and there is considerable disagreement as to whether there is an enhancement in the yield of solid carbon over that obtained with a pure iron catalyst. There are reports claiming that the incorporation of copper into an iron catalyst lowers the rate of formation of carbon during the CO/H_2 reaction.[26] On the other hand, Wachs and co-workers[27] found that there was no change in the rate of carbon deposition when either copper or silver was added to iron. In a more comprehensive study performed by Wielers and co-workers,[28] it was shown that the amount of solid carbon formed on silica supported iron−copper particles during interaction with CO/H_2 (3:1) at 400 °C was very sensitive to the amount of the Group 1B metal present in the bimetallic. When the concentration of copper was about 50% or less than the amount of deposited carbon was greater than that formed on a pure iron catalyst. As the concentration of copper was increased above this level, there was a concomitant decrease in the yield of solid carbon. Here, we focus attention on the carbon deposition reaction on unsupported copper−iron catalysts with particular emphasis being placed on the impact of the bimetallic composition on the structural characteristics of the solid carbon product.

TABLE 1: Solid Carbon Yield (g of carbon/g of catalyst) as a Function of Reaction Temperature from the Decomposition of CO/H_2 (4:1) over Various Fe−Cu Catalysts

catalyst	500 °C	550 °C	600 °C	650 °C	700 °C	750 °C
Fe	11.63	11.56	10.69	9.76	6.67	
Fe−Cu (9:1)	12.20	11.58	10.74	10.12	7.14	
Fe−Cu (7:3)	12.75	11.64	10.44	10.09	7.40	
Fe−Cu (5:5)	10.06	12.47	10.44	9.35	7.00	
Fe−Cu (3:7)	5.90	10.88	10.41	9.18	6.33	
Fe−Cu (1:9)	1.30	5.1	5.7	0.30	3.40	1.30

TABLE 2: Solid Carbon Yield (g of carbon/g of catalyst) as a Function of Reaction Temperature from the Decomposition of CO/H_2 (1:4) over Various Fe−Cu Catalysts

catalyst	500 °C	550 °C	600 °C	650 °C	700 °C	750 °C
Fe	2.19	1.82	2.58	3.80	2.05	
Fe−Cu (9:1)	1.92	1.83	2.64	3.78	2.27	
Fe−Cu (7:3)	1.83	2.22	2.72	3.76	2.39	
Fe−Cu (5:5)	2.02	1.97	2.78	3.65	1.81	
Fe−Cu (3:7)	1.83	2.07	2.67	3.42	1.59	
Fe−Cu (1:9)	0.40	1.0	0.1	0.2	1.50	0.6

Experimental Section

Materials. The powdered copper−iron catalysts were prepared by the coprecipitation method of the metal carbonates from the respective metal nitrates mixed in desired ratios using ammonium bicarbonate at room temperature.[12] The solution was filtered and dried overnight in air at 110 °C and ground to a fine powder. The mixed carbonates were then calcined in air at 400 °C and subsequently reduced in a 10% H_2/He flow for 20 h at 500 °C. Before removing from the reactor, the reduced bimetallic granules were passivated in a 5% air/He stream at room temperature for 1.0 h. This procedure allows for the formation of a thin oxide layer on the granules that prevents sintering due to exothermic reactions upon exposure to air.

The gases used in this work, CO, H_2, and He were all 99.99% purity and were supplied by Air Products Inc. Prior to use the CO was passed through a heating coil maintained at 200 °C, which served as a trap to remove iron carbonyl from the system. All other gases were used without further purification. Reagent grade cupric nitrate [$Cu(NO_3)_2 \cdot 3H_2O$] and ferric nitrate [$Fe(NO_3)_3 \cdot 9H_2O$] were obtained from Fisher Scientific for the catalyst preparations.

Apparatus. Approximately 100 mg of a given powdered bimetallic catalyst sample was evenly dispersed along the base of a ceramic boat that was subsequently positioned in the center of a horizontal quartz reactor tube located in a Lindberg furnace. The catalyst was initially reduced in a 100 cm^3/min of 10%H_2/He flow at 600 °C for 2 h. Following reduction, the temperature was quickly brought to the desired level and the sample reacted in a predetermined mixture of CO and H_2 at a total flow rate of 100 cm^3/min for a period of 2 h. MKS mass flow controllers regulated the gas supplies to the reactor. The reaction was followed as a function of time by sampling both the inlet and outlet gas streams at regular intervals and analyzing the reactants and products by gas chromatography using a 30-m megabore (GS-Q) capillary column in a Varian 3400 GC. At the termination of the carbon deposition reaction, the CO/H_2 flow was switched off and the system allowed to cooled in the presence of He to room temperature. The amount of solid carbon that accumulated on the catalyst was determined by weight difference.

The details of the structural characteristics of the solid carbon products were obtained by a combination of techniques. The overall degree of crystalline perfection was determined from a comparison of the oxidation profiles of individual samples with those of two standard materials, amorphous carbon and graphite, according to a previously described procedure.[29] These measurements were carried out in a Cahn microbalance in the presence of a CO_2/He (9:2) reactant gas mixture. Prior to gasification of the carbon samples, any associated metal catalyst particles were removed by dissolution in 1 M hydrochloric acid over a period of 2 weeks. Failure to perform this step would result in premature oxidation due to the catalytic influence of the metal impurities, hence giving rise to misleading gasification data. X-ray diffraction examinations were performed in a Bruker D5005 powder diffractometer equipped with a nickel monochromator. Diffraction was carried out with Cu Kα radiation at a scan rate of 0.12°/min and peaks were identified by comparison with standards in a PDF database. BET surface area measurements of each solid carbon sample were carried out in a Coulter Omnisorb 100 CX unit with nitrogen at −196 °C using the static flow method.

The structural features of the solid carbon deposit were established from examination in a 2000 EXII transmission electron microscope (lattice resolution = 0.18 nm). Transmission specimens were prepared by ultrasonic dispersion in isobutyl alcohol and application of a drop of the solution onto a holey carbon grid. Inspection of many areas of such specimens revealed that the graphite nanofibers were the exclusive form of material formed in the current experiments conducted at temperatures below 700 °C. High-resolution studies provided information on the arrangement and perfection of the graphite sheets constituting the nanofibers.

Results

Flow Reactor Studies. The effect of the bimetallic catalyst composition on the yields of solid carbon generated from the decomposition of CO/H_2 (4:1) after 2.0 h at various temperatures is presented in Table 1. From these data, it is evident that the amount of solid carbon did not change to any significant degree as the amount of copper was progressively increased to about 70%; however, there was a sharp decrease at higher levels. Examination of the data given in Tables 1 and 2 shows that this trend in solid carbon production was maintained at temperatures up to 700 °C and appeared to be independent of

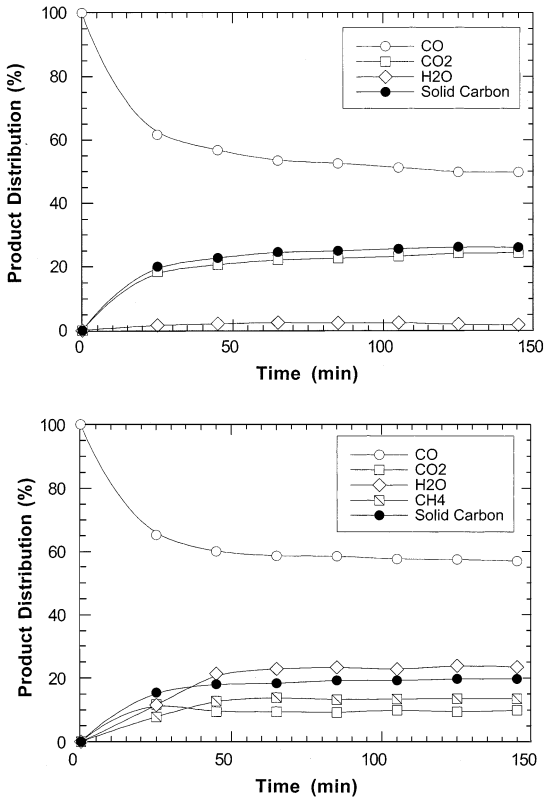

Figure 1. Change in gas-phase product distribution as a function of reaction time for various CO/H_2 mixtures over Fe−Cu (7:3) at 600 °C. These data are calculated by mass balances and the units are moles of product/mol of CO input, (a) $CO:H_2$ (4:1) and (b) $CO:H_2$ (1:4).

the CO/H_2 reactant ratio. Comparison of these results shows that, with the exception of the Fe−Cu (1:9) catalyst composition, the behavior of the majority of the bimetallic powders follows that exhibited by pure iron. It is interesting to find that when the metal powders were exposed to a CO/H_2 (4:1) reactant the maximum yield of solid carbon was obtained at 500 °C. In contrast, when the reaction was conducted with a CO/H_2 (1:4) gas mixture the optimum carbon yield was obtained at 650 °C. Perhaps the most dramatic effect occurs with the Fe−Cu (1:9) catalyst where one observes the existence of two maxima, at 550 and 700 °C. Moreover, this activity profile appears to be independent of the composition of the reactant mixture. Gas-phase product analysis was carried out for the interaction of Fe−Cu (7:3) with CO/H_2 (4:1) and CO/H_2 (1:4) mixtures at 600 °C as a function of reaction time. Inspection of these data, which are presented in Figure 1a,b, highlights the difference in the selectivity patterns exhibited by these two systems.

In a further series of experiments, the influence of hydrogen on the solid carbon formation was determined at 600 °C and the data obtained with an Fe−Cu (7:3) catalyst was compared with that of pure iron when reacted under the same conditions. The data obtained from these two systems are presented in Figure 2, where it can be seen that the dependencies are almost identical, thus indicating that under these circumstances copper does not function as a promoting agent for carbon deposition. Optimum yields of solid carbon are obtained with a reactant mixture containing between 5 and 10% H_2.

Characterization of the Solid Carbon Product. Examination of the solid carbon products by transmission electron microscopy showed that when the synthesis temperature was below 700 °C the deposit consisted entirely of nanofiber structures. At 700 °C, in addition to the fibrous material one

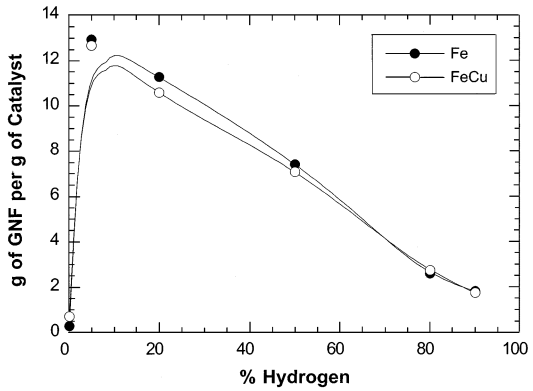

Figure 2. Effect of hydrogen on the amount of solid carbon produced from Fe−Cu (7:3) and pure Fe catalyzed decomposition of CO at 600 °C.

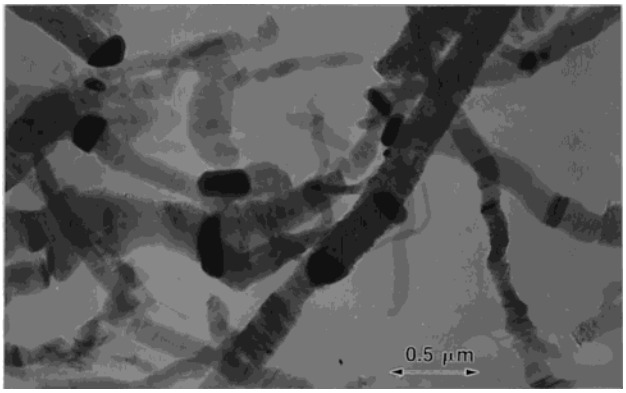

Figure 3. Transmission electron micrograph showing the appearance of nanofibers formed from the interaction of Fe−Cu (7:3) with CO/H_2 (4:1) at 600 °C.

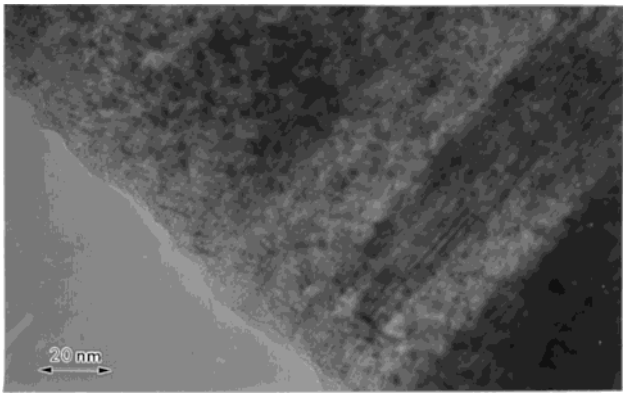

Figure 4. High-resolution electron micrograph of a section of a nanofiber generated from the decomposition of CO/H_2 (4:1) over an Fe−Cu (7:3) catalyst at 600 °C showing the appearance of graphite sheets stacked in a direction perpendicular to the fiber axis.

also observed the presence of "onion-like" structures where the metal catalyst particles appeared to be completely enveloped by graphitic layers. Figure 3 shows the typical appearance of the material produced from the interaction of a CO/H_2 (4:1) mixture with an Fe−Cu (7:3) catalyst at 600 °C. Inspection of this micrograph suggests that the nanofibers were formed by the "whisker type mode" in which the metal catalyst particles remained at the tip of the carbon structures and were carried away from their initial location during the growth process. It is also evident that the electron density is uniform across a given nanofiber, there being no evidence for the formation of a mixed structure. A more detailed understanding of the structure features of the nanofibers was obtained when these samples were

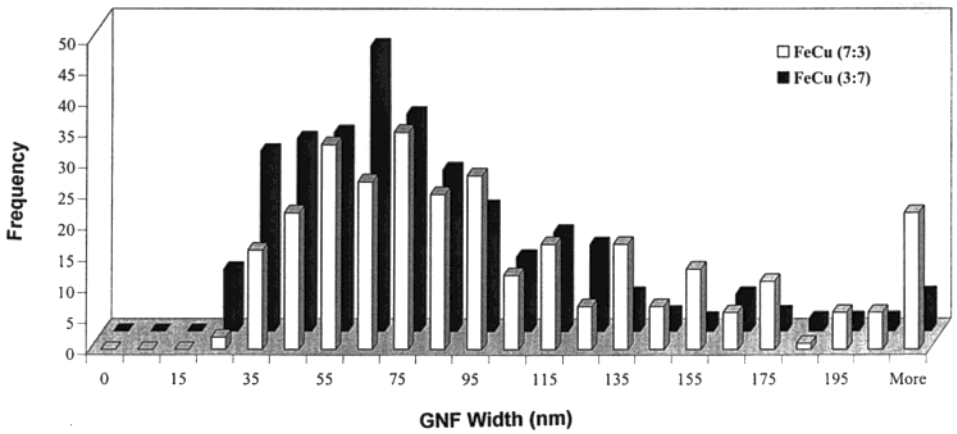

Figure 5. Variation in widths of graphite nanofibers as a function of Fe−Cu catalyst composition during the decomposition of CO/H_2 (4:1) at 600 °C.

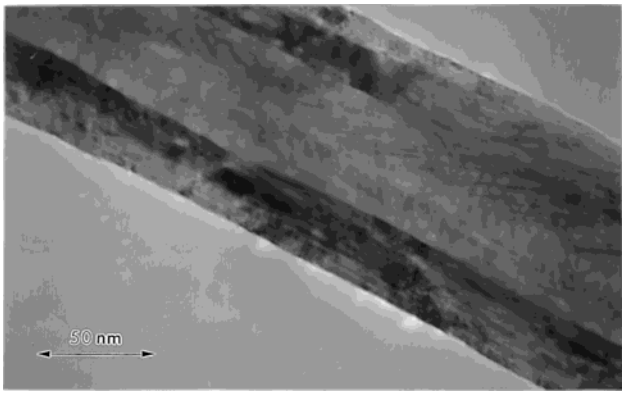

Figure 6. Transmission electron micrograph showing the appearance of nanofibers formed from the interaction of Fe−Cu (7:3) with CO/H_2 (4:1) at 700 °C.

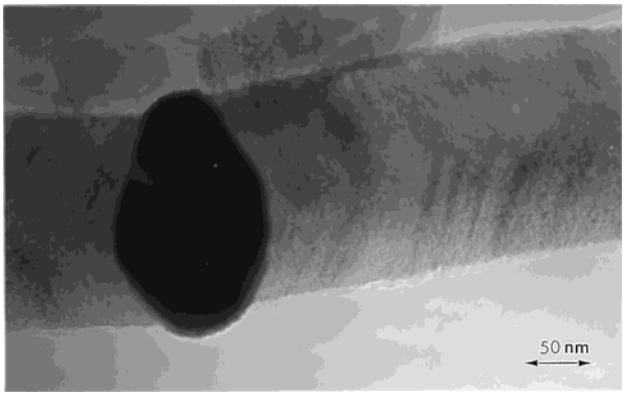

Figure 7. High-resolution electron micrograph of a section of a nanofiber generated from the decomposition of CO/H_2 (1:4) over an Fe−Cu (7:3) catalyst at 600 °C showing the appearance of graphite sheets stacked in a "herringbone" arrangement.

examined at higher resolution, Figure 4. One can see from the lattice fringe images that these materials consist of graphite sheets stacked in a direction perpendicular to the nanofiber growth axis.

Measurements of the sizes of carbon nanofibers produced from the decomposition of CO/H_2 (4:1) at 600 °C showed that the average width was dependent upon the composition of the bimetallic catalyst used to grow the structures. Figure 5 shows the distributions obtained from nanofibers produced from Fe−Cu (7:3) and Fe−Cu (3:7) catalysts from which it is evident that as the copper content is increased there is a concomitant decrease in the average width of the associated carbon nanofibers.

Major changes in the structural features of the nanofibers were observed when the Fe−Cu (7:3) catalyzed decomposition of CO/H_2 (4:1) was performed at 700 °C. As shown in Figure 6, under these conditions the material acquired a duplex structure consisting of graphitic tubular skin surrounding an amorphous carbon core. Treatment of the same bimetallic in a CO/H_2 (1:4) at 600 °C also resulted in a modification of the nanofiber structure over that shown in Figure 3. In this case, while the nanofibers were once again highly crystalline in nature, the graphite sheets adopted a "herringbone" arrangement, Figure 7.

A completely different type of carbon nanofiber structure was formed from the interaction of a CO/H_2 (4:1) mixture with a copper-rich bimetallic catalyst at 600 °C. From Figure 8 it can be seen that in this case the nanofibers do not possess a well-defined structure, but instead consist of disordered carbon and frequently appear to have an electron transparent core. These

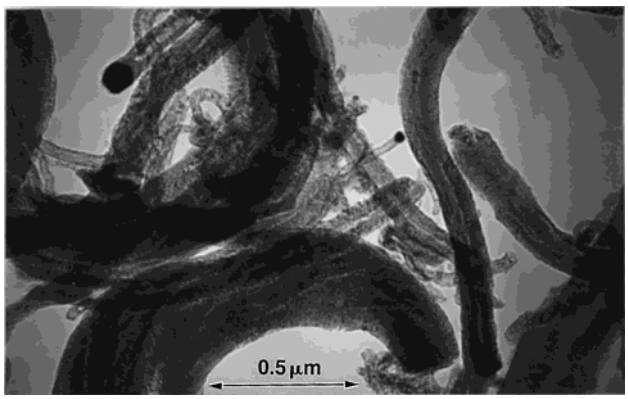

Figure 8. Transmission electron micrograph showing the appearance of nanofibers formed from the interaction of Fe−Cu (1:9) with CO/H_2 (4:1) at 600 °C.

features are clearer in the high-resolution micrograph, Figure 9, where there is no evidence for the formation of graphite sheets within the nanofiber structure.

The temperature programmed oxidation (TPO) profiles for nanofibers formed from the Fe−Cu (7:3) catalyzed decomposition of CO/H_2 (4:1) were determined as a function of reaction temperature and these data are presented in Figure 10. It can be seen that the nanofibers generated between 550 and 650 °C exhibit gasification characteristics that are very close to that of single-crystal graphite.[29] On the other hand, the materials formed at 500 and 700 °C undergo complete gasification at a lower temperature regime, indicating that under these growth condi-

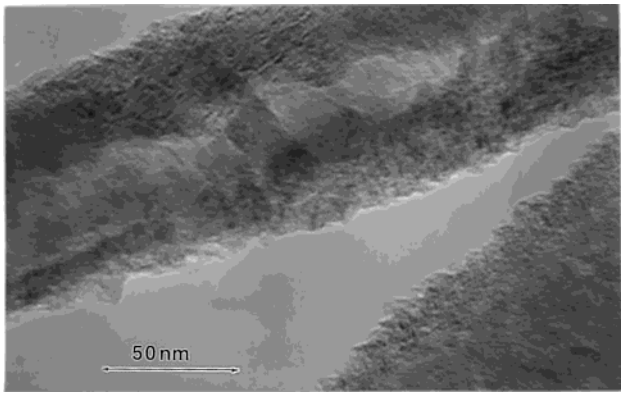

Figure 9. High-resolution electron micrograph of a section of a nanofiber generated from the decomposition of CO/H_2 (4:1) over an Fe−Cu (1:9) catalyst at 600 °C showing the amorphous nature of the material.

tions the structures do not contain any substantial amounts of graphite. The TPO profiles of nanofibers generated from the Fe−Cu (7:3) catalyzed decomposition of CO/H_2 (1:4) are presented in Figure 11 and show that in this case, the products grown at 500 and 700 °C still undergo gasification at lower temperatures than the other materials. A comparison of the profiles indicates that the former structures tend to become more crystalline in nature when grown from a reactant mixture containing excess H_2.

A comparison of the oxidation characteristics of the nanofibers generated from the interactions of all the Fe−Cu bimetallic catalysts with CO/H_2 (4:1) at 600 °C is given in Figure 12. Also included in this plot for comparison purposes are the data obtained from the growth of nanofibers from a pure iron catalyst under the same conditions. Inspection of these profiles reveals that, with the exception of the material grown from Fe−Cu (1:9), the nanofibers generated from the bimetallic catalysts are all more resistant to attack by CO_2 than those formed from pure iron. A similar set of curves was obtained when nanofibers generated from the decomposition of CO/H_2 (1:4) mixtures over

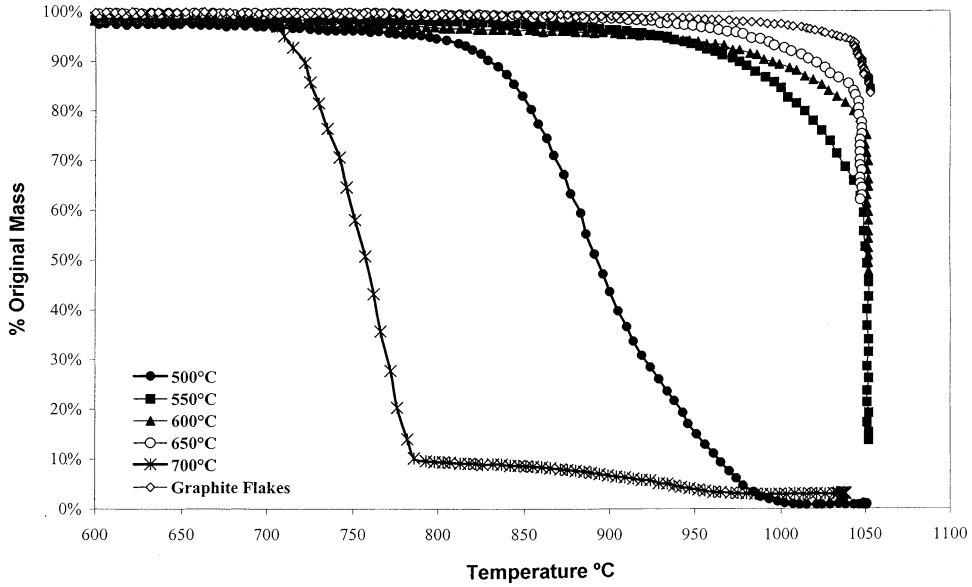

Figure 10. Comparison of the gasification characteristics in CO_2 of nanofibers produced from the interaction of Fe−Cu (7:3) with CO/H_2 (4:1) at temperatures over the range 500−700 °C.

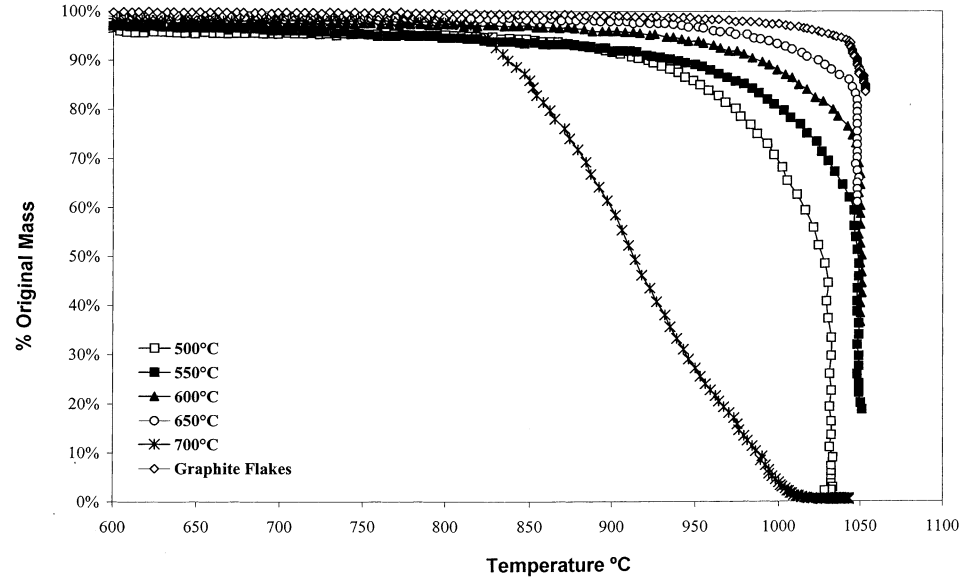

Figure 11. Comparison of the gasification characteristics in CO_2 of nanofibers produced from the interaction of Fe−Cu (7:3) with CO/H_2 (1:4) at temperatures over the range 500−700 °C.

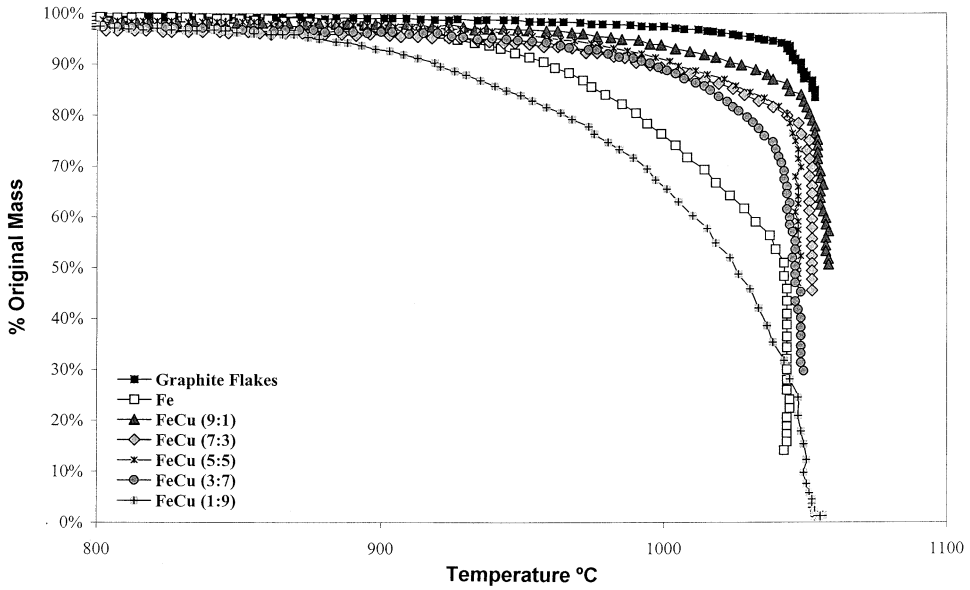

Figure 12. Comparison of the gasification characteristics in CO_2 of nanofibers produced from the interaction of various Fe−Cu powders with CO/H_2 (4:1) at 600 °C. Also included in this plot are the corresponding curves obtained from the gasification of pure graphite under the same conditions.

TABLE 3: X-ray Diffraction Data of Carbon Nanofibers Grown from the Decomposition of CO/H_2 Mixtures over an Fe−Cu (7:3) Catalyst at Various Temperatures

reaction temp (°C)	CO/H_2 ratio	d-spacing (nm)
550	4:1	0.3409
600	4:1	0.3369
650	4:1	0.3359
550	1:4	0.3395
600	1:4	0.3376
650	1:4	0.3361
700	4:1	0.3371
Fe-600	4:1	0.3371
graphite		0.3359

these catalyst systems at 600 °C were subsequently reacted in CO_2. These findings indicate that the introduction of controlled amounts of copper into iron improves the crystalline perfection of the nanofibers produced during the catalyzed decomposition of CO/H_2 mixtures when the reaction is performed at about 600 °C.

X-ray diffraction analysis was carried out on nanofibers grown from the decomposition of CO/H_2 (4:1) and CO/H_2 (1:4) at 600 °C, respectively. The results of these studies, that were determined using a modified Lorentzian curve fitting model, are given in Table 3. Examination of the *d* spacings shows that in both reaction mixtures the nanofibers become more graphitic as the reaction temperature is raised to 650 °C, which is consistent with the TPO curves.

In a final set of experiments, the variation in the surface area of the nanofibers was determined as a function of preparation conditions. It was found that within experimental error values of around 100 m^2/g were obtained from systems in which the bimetallic catalyst composition was less than 70% Cu and above level the nanofibers exhibited a value of about 200 m^2/g. The higher number is consistent with the fact that the material became more disordered when the CO/H_2 reaction was carried out over an Fe−Cu (1:9) catalyst. Figure 13 shows the dependence of the surface areas of nanofibers generated from the Fe−Cu (7:3) catalyzed decomposition of CO/H_2 (4:1) and CO/H_2 (1:4) as a function of reaction temperature. It is evident that a substantial drop in surface area occurs for both reactant mixtures as the growth temperature is increased from 550 to

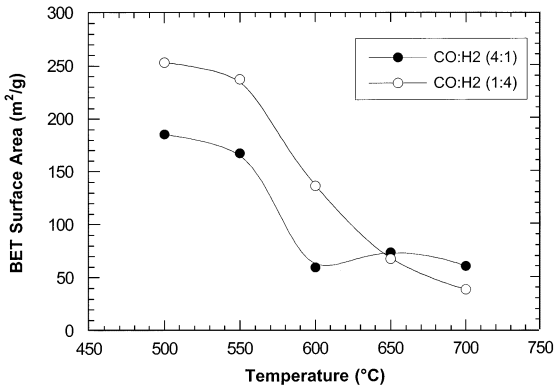

Figure 13. Variation of the surface area of nanofibers produced from the interaction of Fe−Cu (7:3) with CO/H_2 (4:1) and CO/H_2 (1:4), respectively, as a function of temperature.

600 °C and on continued heating remains almost level. It is probable that this trend is directly associated with the tendency of nanofibers to acquire the highest degree of crystalline perfection from a given bimetallic catalyst system at the threshold temperature of 600 °C.

The effect of the catalyst composition on the surface area of nanofibers formed during the decomposition of CO/H_2 (4:1) and CO/H_2 (1:4) mixtures at 600 °C is presented in Figure 14. It is apparent that higher values were obtained from nanofibers generated from the reaction all the bimetallics with the CO/H_2 (1:4) reactant. There did not appear to be any change in the surface areas from either reactant mixtures as the concentration of Cu in the catalyst was increased from 0 to 70%; however, at higher contents there was a substantial increase in the values. These findings are consistent with the TEM observations, which indicated that nanofibers grown from an Fe−Cu (1:9) catalyst were highly amorphous in nature.

Discussion

A comparison of catalyzed solid carbon growth from Fe−Cu/CO−H_2 with that from Fe−Cu/C_2H_4−H_2[4,30] reveals the existence of major differences in the behavior of the two systems. In the latter reaction, the catalytic activity of the single

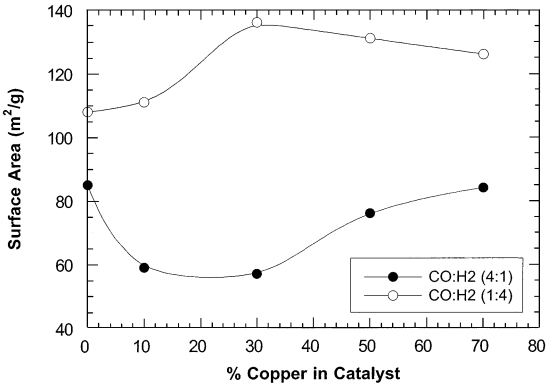

Figure 14. Variation of the surface area of nanofibers produced at 600 °C from the interaction of Fe−Cu with CO/H_2 (4:1) and CO/H_2 (1:4), respectively, as a function of catalyst composition.

metals was very low; however, copious amounts of solid carbon were produced when the C_2H_4/H_2 mixture was passed over a bimetallic. In contrast, when CO/H_2 was used as the reactant the addition of copper to iron did not result in a significant increase in the amount of nanofibers formed over that produced from a pure iron catalyst.

In other experiments, it was found that as the hydrogen content in the C_2H_4/H_2 mixture was increased up to 80% so the amount of solid carbon generated in the system reached an optimum value.[4] In the current investigation, hydrogen was observed to exert the diametrically opposite effect on the carbon deposition characteristics, reaching a maximum yield for a CO/H_2 (9:1) mixture and exhibiting a uniform decrease as the hydrogen content was progressively raised to higher levels. This trend mirrored the dependence found for the generation of solid carbon from the $Fe/CO-H_2$ system[31] and is also consistent with the conclusions reached by Wachs and co-workers.[27]

The progressive decline in the amount of solid carbon formed as the hydrogen content of the reactant was increased can be best understood from a consideration of the gas-phase product distributions, Figure 2a,b. When CO was the dominant reactant then CO_2 was the major gas-phase product and the amount was very close to that of the solid carbon product. Under these conditions, the formation of H_2O and CH_4 was very low. One may therefore conclude that solid carbon is being produced exclusively via the Boudouard reaction ($2CO \rightarrow CO + C_s$). When the reactant mixture contained excess H_2, there was a significant change in the product yields. In this case, H_2O was the primary product, the amount of CH_4 generated increased and exhibited a similar yield pattern to that of CO_2. From these trends, it would appear that the Boudouard reaction was no longer the controlling step, but was now competing with hydrogenation ($CO + H_2 \rightarrow H_2O + C_s$) and methanation ($CO + 3H_2 \rightarrow CH_4 + H_2O$) reactions. Under these latter conditions, the metal particles will rapidly become covered with chemisorbed hydrogen causing CO to interact with the modified surface via the O atom in the molecule. This arrangement will allow the C atom in the CO molecule to form chemical bonds with other hydrogen atoms. The subsequent rupture of the C−O bond in the adsorbed intermediate would generate H_2O and CH_4.[31] Solid carbon would be generated in relatively low amounts along with more H_2O from the hydrogenation reaction.

Other differences are apparent when one examines the structural characteristics of the nanofibers generated from the interaction of the bimetallic with C_2H_4/H_2 and CO/H_2. The onset of gasification in CO_2 of nanofibers formed from the catalyzed decomposition of C_2H_4 was found to commence at temperatures of about 550 °C, indicating that the materials contained a large fraction of disordered carbon. While the addition of H_2 to the reactant mixture did result in an improvement in the oxidation resistance of the solids, the overall degree of crystalline perfection was not very high.[30] In contrast, when CO was used as the source of solid carbon, the nanofibers produced at temperatures over the range 550−650 °C were highly graphitic in nature.

A comparison of the high-resolution electron micrographs of the respective nanofibers grown from the Fe−Cu (7:3) catalyzed decomposition of CO/H_2 (4:1) and C_2H_4/H_2 (4:1) at 600 °C provides an excellent example of how one can manipulate the architecture of the materials by merely changing the nature of the carbon-containing gas. The graphite sheets constituting the structures produced from the olefin were oriented at an angle to fiber axis in a "herringbone" arrangement. When the same bimetallic catalyst was reacted in the presence of CO under otherwise identical conditions, the graphite sheets in the resultant nanofiber product were aligned in a direction perpendicular to the growth axis.

From a consideration of the fundamental aspects involved in the nanofiber growth process, it is apparent that this difference in structure is directly related to the morphological and crystallographic features exhibited by the Fe−Cu catalyst particles in C_2H_4/H_2 and CO/H_2 environments, respectively.[1] In a previous investigation, it was suggested that the C_2H_4 molecule adsorbed in a configuration where the C═C bond in the molecule was aligned in a direction parallel to the bimetallic surface. This process requires the olefin to encounter two surface iron atoms where the separation distance matches that of C═C in the molecule. This condition will facilitate the subsequent rupture of the C═C bond eventually leading to the formation of a carbon nanofiber.[4]

The presence of coadsorbed H_2 appears to be an essential prerequisite for the subsequent dissociative chemisorption of CO on an iron-containing surface.[32−34] From a compilation of the data reported in many surface science papers, it becomes evident that in the presence of CO/H_2 mixtures iron surfaces will undergo reconstruction to form several different faces that can catalyze a various reactions at the same time. Geus and co-workers[35,36] used a variety of techniques including Auger electron spectroscopy and low energy electron diffraction to investigate the interactions of CO with iron surfaces. They concluded that CO would only undergo dissociative chemisorption on iron clusters and not on single iron atoms. On the basis of these findings, it is reasonable to assume that in copper-rich bimetallic particles the iron component is probably in a highly dispersed state, and consequently the chances of the CO molecules encountering clusters of the metal are remote. Under such conditions, the yield of carbon nanofibers will exhibit a sharp decrease and the structural characteristics of such materials is expected to be quite different to those grown from iron-rich catalyst particles.

The modification in structure of the nanofibers produced from the interaction of Fe−Cu (7:3) with CO/H_2 mixtures as the temperature was raised from 600 to 700 °C is most probably associated with the α-Fe to γ-Fe phase change. During this transformation the crystal structure of the metal changes from BCC to FCC, and there is also a major alteration in the carbon solubility and bulk diffusion parameters.[37] Previous studies performed in the controlled atmosphere electron microscopy showed that when iron/graphite samples were heated from 550 to 750 °C in acetylene the metal underwent conversion from α-Fe to the γ-Fe phase. During this temperature excursion, there

was a change in the both the growth kinetics and structural characteristics of carbon nanofibers.[38]

References and Notes

(1) Rodriguez, N. M.; Chambers, A.; Baker, R. T. K. *Langmuir* **1995**, *11*, 3862.
(2) Kim, M. S.; Rodriguez, N. M.; Baker, R. T. K. *J. Catal*. **1991**, *131*, 60.
(3) Chambers, A.; Rodriguez, N. M.; Baker, R. T. K. *J. Phys. Chem.* **1995**, *99*, 10581.
(4) Krishnankutty, N.; Rodriguez, N. M.; Baker, R. T. K. *J. Catal*. **1996**, *158*, 217.
(5) Kim, M. S.; Woo, W. J.; Song, H. S.; Lee, Y. S.; Lee, J. C. *Han'guk Seramik Hakhoechi (Korean)* **2000**, *37*, 345.
(6) Schwab, G. M. *Discuss. Faraday Soc*. **1950**, *8*, 166.
(7) Dowden, D. A.; Reynolds, P. *Discuss. Faraday Soc*. **1950**, *8*, 184.
(8) Hall, W. K.; Emmett, P. H. *J. Phys. Chem.* **1958**, *62*, 816.
(9) Kiskinova, M.; Goodman, D. W. *Surf. Sci*. **1981**, *105*, L265.
(10) Kiskinova, M.; Goodman, D. W. *Surf. Sci*. **1981**, *108*, 64.
(11) Rodriguez, J. A.; Goodman, D. W. *J. Phys. Chem*. **1991**, *95*, 4196.
(12) Best, R. J.; Russell, W. W. *J. Am. Chem. Soc*. **1954**, *76*, 838.
(13) Van der Plank, P.; Sachtler, W. M. H. *J. Catal.* **1968**, *12*, 35.
(14) Ponec, V.; Sachtler, W. M. H. *J. Catal*. **1972**, *24*, 250.
(15) Sinfelt, J. H.; Carter, J. L.; Yates, D. J. C. *J. Catal*. **1972**, *24*, 283.
(16) Takasu, Y.; Yamashina, T. *J. Catal*. **1973**, *28*, 174.
(17) Nishiyama, Y.; Tamai, Y. *J. Catal*. **1974**, *33*, 98.
(18) Araki, M.; Ponec, V. *J. Catal.* **1976**, *44*, 430.
(19) Martin, G. A.; Dalmon, J. A. *J. Catal*. **1982**, *75*, 233.
(20) Modak, S.; Khanra, B. C. *Surf. Sci*. **1988**, *199*, 361.
(21) Harberts, J. C. M.; Bourgonje, A. F.; Stephan, J. J.; Ponec, V. *J. Catal*. **1977**, *47*, 92.
(22) Cale, T. S.; Richardson, J. T. *J. Catal*. **1983**, *79*, 378.
(23) Rodriguez, N. M.; Kim, M. S.; Baker, R. T. K. *J. Catal*. **1993**, *140*, 16.
(24) Baker, R. T. K. *Carbon* **1989**, *27*, 315 1989.
(25) Rodriguez, N. M. *J. Mater. Res*. **1993**, *8*, 3233.
(26) Anderson, R. B. In *Catalysis*; Emmett, P. H., Ed.; Reinhold: New York; Vol. 4, p 1.
(27) Wachs, I. E.; Dwyer, D. J.; Iglesia, E. *Appl. Catal*. **1984**, *12*, 201.
(28) Wielers, A. F. H.; Koebrugge, G. W.; Geus, J. W. *J. Catal*. **1990**, *121*, 375.
(29) Owens, W. T.; Rodriguez, N. M.; Baker, R. T. K. *J. Phys. Chem*. **1992**, *96*, 5048.
(30) Krishnankutty, N.; Park, C.; Rodriguez, N. M.; Baker, R. T. K. *Catal. Today* **1997**, *37*, 295.
(31) Rodriguez, N. M.; Kim, M. S.; Baker, R. T. K. *J. Catal*. **1993**, *144*, 93.
(32) Dry, M. E.; Shingles, T.; Boschoff, L. J.; Van Botha, H. C. S. *J. Catal*. **1970**, *17*, 347.
(33) Benziger, J. B.; Madix, R. J. *Surf. Sci*. **1982**, *115*, 279.
(34) Burke, M. L.; Madix, R. J. *Surf. Sci*. **1990**, *237*, 20.
(35) Vreeburg, R. J.; van de Loosdrecht, J.; Gijzeman, O. L. J.; Geus, J. W. *Catal. Today* **1991**, *10*, 329.
(36) Vink, T. J.; Gijzeman, O. L. J.; Geus, J. W. *Surf. Sci*. **1985**, *150*, 14.
(37) Smith R. P. *AIME Trans.* **1964**, *230*, 476.
(38) Baker, R. T. K.; Chludzinski, J. J.; Lund, C. R. F. *Carbon* **1987**, *25*, 295.